Small molecule regulators of autophagy identified by an image-based high-throughput screen

Lihong Zhang*, Jia Yu*, Heling Pan*, Ping Hu*, Yan Hao*, Wenqing Cai*, Hong Zhu†, Albert D. Yu†, Xin Xie‡, Dawei Ma*§, and Junying Yuan†§

*State Key Laboratory of Bioorganic and Natural Products Chemistry, Shanghai Institute of Organic Chemistry, Chinese Academy of Sciences, 354 Fenglin Road, Shanghai 200032, China; †Department of Cell Biology, Harvard Medical School, 240 Longwood Avenue, Boston, MA 02115; and ‡National Center for Drug Screening, 189 Guoshoujing Road, Shanghai 201203, China

Communicated by Tom A. Rapoport, Harvard Medical School, Boston, MA, October 12, 2007 (received for review September 28, 2007)

Autophagy is a lysosome-dependent cellular catabolic mechanism mediating the turnover of intracellular organelles and long-lived proteins. Reduction of autophagy activity has been shown to lead to the accumulation of misfolded proteins in neurons and may be involved in chronic neurodegenerative diseases such as Huntington's disease and Alzheimer's disease. To explore the mechanism of autophagy and identify small molecules that can activate it, we developed a series of high-throughput image-based screens for small-molecule regulators of autophagy. This series of screens allowed us to distinguish compounds that can truly induce autophagic degradation from those that induce the accumulation of autophagosomes as a result of causing cellular damage or blocking downstream lysosomal functions. Our analyses led to the identification of eight compounds that can induce autophagy and promote long-lived protein degradation. Interestingly, seven of eight compounds are FDA-approved drugs for treatment of human diseases. Furthermore, we show that these compounds can reduce the levels of expanded polyglutamine repeats in cultured cells. Our studies suggest the possibility that some of these drugs may be useful for the treatment of Huntington's and other human diseases associated with the accumulation of misfolded proteins.

rapamycin | light chain 3 | PI3P

Autophagy is a cellular catabolic mechanism mediating the turnover of intracellular organelles and proteins through a lysosome-dependent but proteasome-independent degradative pathway (1, 2). An autophagosome sequesters cytoplasmic constituents, such as mitochondria, endoplasmic reticulum, and ribosomes, by forming a double-membrane vesicle. The outer membrane of the autophagosome then fuses with the lysosome in mammalian cells delivering the sequestered content to the lumen of lysosome for degradation. Autophagy is critical for the survival of yeast and mammalian cells under starvation conditions because it functions to recycle intracellular material for macromolecular synthesis and energy production (3).

Autophagy occurs in all cells at low basal levels under normal conditions to perform homeostatic functions, but it can be rapidly up-regulated under starvation or stress conditions (3). Elegant genetic analysis has identified 17 genes that are essential for autophagy in yeast (referred to as the *ATG* genes) (4, 5). In mammalian cells, mTOR kinase, the target of rapamycin, mediates the major inhibitory signal that shuts off autophagy under nutrient-rich conditions (3). On the other hand, mammalian type III PI3-kinase, the homolog of yeast VPS34 and inhibitable by 3-methyladenine (3-MA) (a nonspecific inhibitor of PI3-kinase), is required for the onset of autophagy. In this regard, rapamycin and 3-MA, the most commonly used chemicals to induce and inhibit autophagy, respectively, provide convenient tools to study autophagy.

To explore the mechanism of autophagy and identify additional small molecules that can activate it, we developed a high-throughput image-based screen. This system takes advantage of the localization of light chain 3 coupled to GFP (LC3-GFP) to the autophagosomal membrane upon induction of autophagy (6). Mammalian LC3, the ortholog of yeast ATG8, has been shown to mark the autophagosome membrane specifically. The number of LC3-GFP-positive autophagosomes per cell is very low under normal growth conditions but is rapidly increased upon serum starvation or the addition of rapamycin (7). Other compounds that increase the cellular levels of LC3-GFP, however, are not necessarily able to increase the degradative activities of autophagy. Instead, the increases of LC3-GFP may be associated with cell death or may be the result of lysosomal defects and thus associated with the blockage of autophagy. Furthermore, because many compounds may affect more than one cellular target, the information on the known targets of compounds is not necessarily useful for identifying those that may influence the activity of autophagy. To overcome these limitations, we developed a series of image-based screens and assay criteria for selecting compounds that regulate autophagy. When coupled with an assay for long-lived protein degradation, these assays allowed us to distinguish compounds that can truly induce autophagic degradation from those that increase the levels of LC3-GFP as a result of causing cellular damage or blocking downstream lysosomal functions. Using this series of image-based screens, we analyzed 480 compounds in the ICCB known bioactive library (BIOMOL). Our analyses led to the identification of eight compounds that can induce autophagy and promote long-lived protein degradation without causing obvious cellular injury.

Results

An Image-Based Screen for Inducers of Autophagy. We established a human glioblastoma H4 cell line stably expressing human microtubule-associated protein (MAP) LC3-GFP. As reported previously (7), LC3-GFP specifically marks the autophagosomal membrane, and thus, each LC3-GFP spot represents an individual autophagosome. H4-LC3-GFP cells were cultured in 96-well plates and incubated individually with 480 compounds in a known bioactive compound library (BIOMOL catalog 2840; www.biomol.com) at concentrations of 3–12 μM, with the exception of rapamycin (0.22 μM) and bafilomycin A1 (0.40 μM) for 24 h. The levels of autophagy were analyzed with LC3-GFP as a marker by measuring the number, size, and intensity of LC3-GFP spots with high-throughput fluorescent microscopy. DMSO and rapamycin were used as negative and positive controls, respectively.

Author contributions: J. Yu and H.P. contributed equally to this work; D.M. and J. Yuan designed research; L.Z., J. Yu, H.P., P.H., Y.H., W.C., and H.Z. performed research; L.Z., H.P., A.D.Y., X.X., and J. Yuan analyzed data; and L.Z., D.M., and J. Yuan wrote the paper.

The authors declare no conflict of interest.

§To whom correspondence may be addressed. E-mail: madw@mail.sioc.ac.cn or jyuan@hms.harvard.edu.

This article contains supporting information online at www.pnas.org/cgi/content/full/0709695104/DC1.

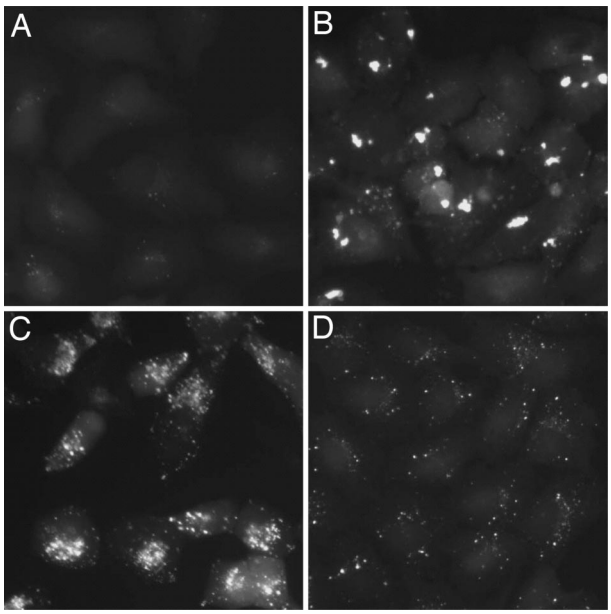

Fig. 1. Typical morphological changes of autophagosome. H4-LC3-GFP cells were treated with DMSO (*A*), grayanotoxin III (*B*), bafilomycin A1 (*C*), and rapamycin (*D*) for 24 h, and the images were analyzed by fluorescence microscopy. The concentrations of the compounds were the same as that used in the screening (SI Table 4).

We found that the treatment of H4 cells with 72 of 480 known bioactive compounds led to a >50% increase in the fluorescence levels of LC3-GFP compared with DMSO control-treated cells [supporting information (SI) Table 4]. This screen identified rapamycin and tamoxifen, two known activators of autophagy, as having an increasing effect on the levels of LC3-GFP (7, 8). This screen also identified inhibitors of lysosomal function, such as bafilomycin A1, a vacuolar ATPase inhibitor, which is known to increase the numbers of intracellular autophagosomes by blocking the ability of the lysosome to degrade autophagosome. The compounds that can change intracellular pH, such as nigericin or monensin, which are known to be capable of blocking lysosomal (i.e., methylamine-sensitive) protein degradation in isolated rat hepatocytes (9), also led to an increase effect in the levels of LC3-GFP. These results suggest that this LC3-GFP-based image screen is able to identify the compounds that increase the levels of autophagy.

We noted that the cells treated with different compounds exhibited distinct characteristics in the morphology and intracellular distributions of autophagosomes as marked by the size, intensity, and distribution of LC3-GFP$^+$ vesicles. Such changes can be categorized into three groups based on the features of the LC3-GFP$^+$ vesicles (Fig. 1). However, because the effects of the compounds on the sizes and distributions of the LC3-GFP$^+$ vesicles may exhibit dynamic changes during incubation, we chose to only provide images of typical changes noted, rather than a complete classification of all of the compounds analyzed.

Type 1. Compounds that may have a more profound effect on the surface area and intensity of an individual LC3-GFP$^+$ vesicle than on the total number are classified as type1. Grayanotoxin III, a member of a family of toxic diterpenoids found in Rhododendron species and an activator of voltage-sensitive sodium channels, is such an example (Fig. 1 *A* and *B*).

Type 2. Compounds that may not only increase the surface area and intensity of LC3-GFP$^+$ vesicles but also lead to the aggregation of LC3-GFP$^+$ vesicles around the nuclear membrane (Fig. 1*C*) are classified as type 2. Many compounds that have influence on the lysosomal functions, e.g., monensin and bafilomycin A1, belong to this class, suggesting that such compounds may cause the accumulation of autophagosomes by blocking the downstream lysosomal pathway and/or intracellular trafficking of autophagosomes. Consistent with this hypothesis, wiskostatin, an inhibitor of *N*-WASP and actin dynamics, belongs to this class.

Type 3. Compounds that may increase the number, individual surface area, and intensity of LC3-GFP$^+$ vesicles (Fig. 1*D*) are classified as type 3. Rapamycin, a known activator of autophagy and immunosuppressant compound that inhibits the mTOR complex 1 (mTORC1) in the mTOR pathway, is such an example (Fig. 1). In addition, the treatment with tamoxifen, an estrogen antagonist and known activator of autophagy, also led to similar changes in the LC3-GFP$^+$ vesicles (data not shown). Because two known activators of autophagy, rapamycin and tamoxifen, both belong to this class, we expected that at least some of the compounds that increase number, individual surface, area and intensity of LC3-GFP$^+$ vesicles can truly activate the autophagic degradation.

Whereas the induction of LC3-GFP$^+$ vesicles by some of the compounds was accompanied by cell death, others induced autophagy without obvious effects on cell viability. Specifically, 23 compounds listed in the SI Table 4 were found to induce significant toxicity as indicated by >30% of reduction in the cell numbers based on nuclear counterstain with 4,6-diamidino-2-phenylindole (DAPI) after the treatment for 24 h as analyzed by high-throughput microscopy. One such example was trichostatin A, a histone deacetylase inhibitor, consistent with an earlier report that histone deacetylase inhibitors are capable of causing autophagic cell death (10). Thapsigargin, an inhibitor of sarco/endoplasmic reticulum Ca^{2+} ATPase, also induced autophagy associated with a reduction in the cell number. Thapsigargin induces endoplasmic reticulum (ER) stress by disrupting intracellular Ca^{2+} homeostasis, and ER stress is known to induce autophagy (11), possibly as a compensatory regulatory mechanism. Because the goal of this project was to identify compounds that truly induce autophagic degradation without causing significant cell death, we removed the compounds associated with >30% reduction of cell numbers from further analysis. The subsequent analysis concentrated on 47 compounds that can induce an increase in the levels of LC3-GFP without significant loss of cell viability in 24 h (marked with * in SI Table 4).

Effects of Compounds on the Intracellular Phosphatidylinositol 3-Phosphate [PtdIns(3)*P*]. Although we still understand very little about the molecular mechanisms that regulate autophagy beyond starvation, autophagy has been shown to be activated in response to a variety of extracellular and intracellular stresses, including nutrient deprivation, bacterial infection, misfolded proteins, and damaged organelles. Many intracellular signaling molecules, such as AMP-activated protein kinase (AMPK), mTOR, Class I PI3K, MAPK, are implicated in the regulation of autophagy (12). In addition, Ca^{2+} and Ca^{2+}-regulated proteases, calpains (13), and calmodulin (11) may also be involved. Our task, therefore, is to distinguish compounds that can truly accelerate autophagic degradation by regulating the activities of molecules involved in autophagy from those that induce autophagy as a result of causing cellular injury. Because compounds may have unintended effect(s) on multiple protein targets, the known target of a given compound is not necessarily informative when deciding whether this compound can be a true inducer of autophagic degradation. We decided to use a series of additional image-based screens to develop a set of criteria that would allow us to identify selective inducers of autophagy.

PtdIns(3)*P*, formed by the phosphorylation of phosphatidylinositol by the class III PI3-kinases, is crucial for endocytic and autophagic membrane traffic (14). Vps34/beclin1, the mammalian homologs of yeast type III PI3-kinase complex, are essential for autophagy (15). We reason that because PtdIns(3)*P* is

Table 1. Compounds that increase the levels of FYVE-RFP

Name	% of control FYVE-RFP spot intensity per cell		
	2 h	4 h	8 h
Rapamycin	164.93 ± 10.96	131.41 ± 26.64	152.35 ± 4.55
Nigericin	148.43 ± 5.17	145.40 ± 8.39	140.54 ± 18.21
Wiskostatin	267.90 ± 6.16	240.08 ± 4.26	131.93 ± 11.05
Fluspiriline	224.98 ± 16.90	142.15 ± 5.77	108.53 ± 6.07
Niguldipine	147.18 ± 25.39	148.26 ± 3.67	125.53 ± 2.84
Trifluoperazine	136.58 ± 15.74	111.52 ± 13.45	94.28 ± 2.87
Nicardipine	132.05 ± 19.93	112.51 ± 10.09	104.77 ± 31.63
Penitrem A	121.40 ± 12.66	87.41 ± 5.90	72.71 ± 5.57

The levels of FYVE-RFP were measured at 2, 4, and 8 h after the compound addition as described in *Methods* and expressed as a percentage of that of control DMSO-treated cells.

Table 2. Compounds that have no effect on the levels of FYVE-RFP

Name	% of control FYVE-RFP spot intensity per cell		
	2 h	4 h	8 h
Tamoxifen	77.66 ± 4.43	71.55 ± 0.73	85.37 ± 7.59
Loperamide	115.39 ± 5.20	123.62 ± 1.37	95.70 ± 12.84
Amiodarone	92.50 ± 5.51	89.23 ± 3.47	83.45 ± 3.64
Pimozide	94.42 ± 4.71	103.96 ± 9.06	73.64 ± 12.18
Clozapine	64.04 ± 2.94	74.79 ± 13.43	78.38 ± 1.35
Cyclopamine	108.75 ± 12.44	75.21 ± 1.18	96.38 ± 5.12
Paxilline	100.56 ± 0.58	52.37 ± 1.65	56.82 ± 4.44
FPL-64176	99.43 ± 9.62	78.17 ± 1.90	87.62 ± 2.42
Verapamil	83.96 ± 20.67	70.15 ± 13.00	71.28 ± 11.29
Propafenone	114.69 ± 8.90	78.75 ± 18.93	62.87 ± 3.38
Bay K-8644	110.18 ± 25.18	57.79 ± 3.76	79.70 ± 7.28
Quinine	70.35 ± 10.23	78.03 ± 6.33	60.70 ± 6.59
SDZ-201106	65.87 ± 4.72	59.79 ± 2.38	72.40 ± 20.27
TMB-8	89.59 ± 4.79	74.72 ± 13.74	78.64 ± 10.26
Cyclosporin A	73.62 ± 5.70	71.69 ± 27.87	55.82 ± 4.16
NapSul-Ile-Trp-CHO	89.37 ± 3.52	64.10 ± 11.47	62.34 ± 8.21
CA-074-Me	65.94 ± 12.73	79.82 ± 4.66	86.43 ± 4.15
Ac-Leu-Leu-Nle-CHO	72.86 ± 10.18	84.85 ± 2.83	88.42 ± 6.29
CAPE	86.89 ± 20.98	71.17 ± 18.70	69.14 ± 4.32
H9	102.35 ± 12.94	79.63 ± 1.52	83.01 ± 6.62
K252A	76.86 ± 6.51	65.58 ± 9.36	70.33 ± 5.89
AM 92016	68.06 ± 1.20	71.97 ± 15.67	66.35 ± 17.66

The procedure was the same as that in Table 1.

essential for autophagy, compounds that truly induce autophagic degradation should not lead to a reduction in the levels of PtdIns(3)*P*.

The FYVE domain is a conserved ≈70-residue zinc finger protein domain that binds PtdIns(3)*P* with high specificity (16). The interactions of PtdIns(3)*P* with the FYVE domains in different proteins have been shown to function in regulating membrane dynamics and protein trafficking. Fluorescent-labeled FYVE domains have been used as a marker for the levels and location of intracellular PtdIns(3)*P* (17). To analyze the effect of compounds on the intracellular levels of PtdIns(3)*P*, we established an H4 cell line expressing FYVE-RFP. As reported previously, the treatment with rapamycin led to an increase in the levels of FYVE-RFP$^+$ vesicles (Table 1). On the other hand, the treatment with tamoxifen, another known inducer of autophagy, did not lead to any significant change in the levels of FYVE-RFP spots (Table 2). As a negative control, the treatment with LY-294002, a PI3-kinase inhibitor, led the reduction in the levels of FYVE-RFP$^+$ vesicles (SI Table 5).

We analyzed the effects of the 47 compounds determined not to cause cellular toxicity (marked with * in SI Table 4) on the levels of FYVE-RFP$^+$ vesicles in H4 cells. We classified the compounds into three classes: compounds that led to increases (Table 1), no change (Table 2), or decreases (SI Table 5) in the levels of FYVE-RFP$^+$ vesicles, respectively. We reason that because PtdIns(3)*P* is essential for autophagic degradation, the compounds that induce autophagic vesicles associated with a reduction of PtdIns(3)*P* levels as marked by a reduction in the FYVE-RFP$^+$ vesicles are likely inducing LC3-GFP by causing intracellular damage. Thus, the 21 compounds that led to the reduction of FYVE-RFP$^+$ vesicles (SI Table 5) may be unlikely to induce autophagic degradation. This hypothesis was further tested experimentally below.

Compounds That Promote the Degradation of Long-Lived Proteins. Autophagy mediates the turnover of intracellular long-lived proteins (5). To identify compounds that truly induce autophagy, we analyzed the effects of the 47 nontoxic compounds (marked with * in SI Table 4 and see *SI Methods*) on long-lived protein degradation. Our control experiment indicated that the long-lived protein degradation assay alone had no effect on autophagy as indicated by no changes in the levels of LC3II/LC3I compared with the control cells (data not shown). This analysis identified eight compounds, including fluspirilene, trifluoperazine, pimozide, niguldipine, nicardipine, amiodarone, loperamide, and penitrem A, that can significantly increase the rate of long-lived protein degradation (Table 3 and SI Table 6). Interestingly, most of the compounds that increased the levels of FYVE-RFP$^+$ vesicles indeed also promoted the degradation of long-lived

Table 3. Compounds that increase long-lived protein degradation

Name	% of control long lived protein degradation			
	1 h	2 h	4 h	24 h
Rapamycin	159.89 ± 11.46	171.67 ± 10.41	149.89 ± 24.83	165.87 ± 4.08
Fluspirilene	93.82 ± 3.25	143.17 ± 4.26	144.79 ± 9.02	145.50 ± 2.98
Trifluoperazine	76.62 ± 2.32	105.60 ± 5.01	109.00 ± 5.22	124.78 ± 2.05
Pimozide	129.13 ± 11.46	155.80 ± 9.22	152.01 ± 9.63	162.47 ± 3.50
Nicardipine	84.62 ± 4.48	126.59 ± 3.83	122.60 ± 7.70	121.03 ± 13.43
Penitrem A	92.88 ± 2.83	126.09 ± 0.47	132.13 ± 10.01	141.83 ± 1.25
Niguldipine	71.65 ± 2.68	107.42 ± 2.72	105.68 ± 2.74	117.85 ± 1.98
Loperamide	78.70 ± 13.17	122.10 ± 6.48	125.21 ± 4.29	139.19 ± 18.77
Amiodarone	101.32 ± 5.95	122.42 ± 9.71	110.75 ± 3.68	116.73 ± 5.54

The rates of long-lived protein degradation were measured as described in *Methods*. The percentages of change were expressed by dividing the rate of degradation in compound-treated cells by that of DMSO-treated cells.

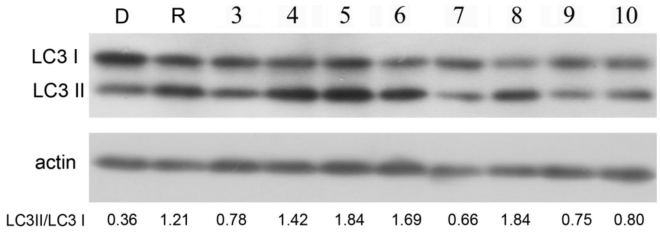

Fig. 2. Effects of compounds on the ratio of LC3II to LC3I. H4 cells were treated with the indicated compounds for 4 h. The cell lysates were harvested and analyzed with Western blotting and anti-LC3 antibody. Anti-actin was used as a loading control. The LC3II/LC3I ratio was quantified. The presented result is a representative of three independent experiments. D, DMSO; R, rapamycin; 3, amiodarone; 4, niguldipine; 5, trifluoperazine; 6, loperamide; 7, penitrem A; 8, pimozide; 9, fluspiriline; 10, nicardipine. The concentrations of the compounds were the same as that used in the screening (SI Table 4).

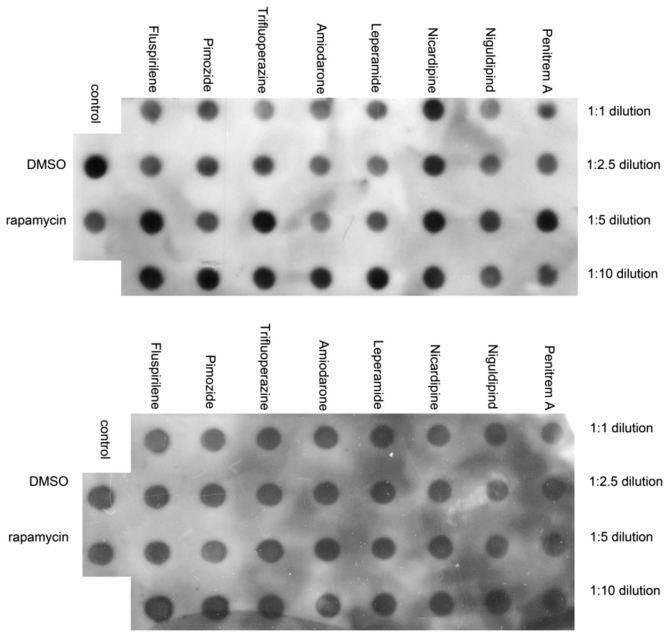

Fig. 3. Effect of compounds on the accumulation of expanded polyglutamine. H4 cells were transiently transfected with an EGFP-Q79-HA expression vector (19). Six hours after the transfection, media were changed, and the compounds were added. After an additional 24 h of incubation, the cells were harvested for analysis of the levels of poly(Q) by dot blotting with anti-HA antibody (*Upper*). Anti-actin antibody was used as a loading control (*Lower*). DMSO and rapamycin were used as negative and positive controls, respectively. The I concentrations of the compounds were the same as that used in the screening (SI Table 4).

proteins (Table 1). Additionally, a few compounds that did not change the levels of FYVE-RFP$^+$ vesicles (Table 2) were also able to promote the degradation of long-lived proteins. Finally, consistent with our hypothesis that class III PI3-kinase activity is necessary for the induction of autophagy, none of the compounds that led to a reduction in the levels of FYVE-RFP$^+$ vesicles promoted the degradation of long-lived proteins.

To further verify the effects of the eight compounds listed in Table 3 on the induction of autophagic degradation, we determined the effects of these compounds on the ratio of LC3II/LC3I, a well established biochemical assay for the activation of autophagy (7). H4 cells were treated with compounds individually and analyzed for the levels of LC3II and LC3I by Western blotting with anti-LC3 antibody. As expected, the treatment with these eight compounds led to significant increases in the ratio of LC3II/LC3I (Fig. 2). From these results, we conclude that we have identified eight compounds, fluspirilene, trifluoperazine, pimozide, niguldipine, nicardipine, amiodarone, loperamide, and penitrem A, that can truly induce autophagic degradation without causing obvious cellular damage.

Effects of Compounds on the Accumulation of Mutant Polyglutamine. The accumulation of misfolded proteins is a hallmark of multiple human chronic neurodegenerative diseases exemplified by polyglutamine expansion diseases such as Huntington's disease, and activation of autophagy has been proposed as a mechanism to enhance the clearance and reduce the accumulation of misfolded proteins (18). To examine whether the eight autophagy inducers that we have identified can reduce the accumulation of misfolded proteins, we tested the effects of these compounds on the accumulation of poly(Q). H4 cells were transiently transfected with a GFP-Q79-HA construct (19) and treated with compounds individually. Interestingly, the treatment of eight autophagy inducers, with the possible exception of nicardipine, reduced the accumulation of expanded polyglutamine in a dose-dependent manner, as indicated by the reduction of anti-HA signal on the dot blots (Fig. 3). From these results, we conclude that we have identified an interesting set of compounds that can reduce the accumulation of misfolded proteins by promoting autophagic degradation.

Effects of Compounds on the Activation of mTOR. mTOR is a member of the PI3-kinase-related kinase (PIKK) family and a central modulator of cell growth in response to environmental signals (20). mTOR plays a critical role in transducing proliferative signals mediated through the PI3-kinase/Ser/Thr protein kinase B/Akt signaling pathway by activating downstream protein kinases that are required for both ribosomal biosynthesis and translations. By targeting mTOR, rapamycin mimics the cellular starvation response by inhibiting signals required for cell cycle progression, cell growth, and proliferation and leads to activation of autophagy (21). To explore whether any of the autophagy inducers that we have identified might function similarly to rapamycin by inhibiting mTOR, we examined the phosphorylation of mTOR in cells treated with these compounds. As shown in Fig. 4, the treatment of rapamycin led to the dephosphorylation of mTOR as reported; on the other hand, the phosphorylation status of mTOR in cells treated with any of the eight compounds was not altered compared with that of control. Thus, we conclude that we have identified eight compounds that induce autophagy through mechanism(s) distinct from that of rapamycin.

Discussion

In this work, we describe the development of image-based assays coupled with a long-lived protein degradation assay to identify compounds that regulate autophagy. Using these image-based assays, we identified eight compounds that can promote autophagy. The ability of these eight compounds to promote autophagy was validated by using cellular assays of long-lived protein degradation

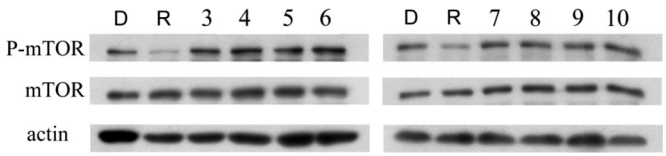

Fig. 4. Effects of compounds on mTOR. H4 cells were treated with the indicated compounds for 4 h. The cell lysates were harvested and analyzed with Western blotting and anti-phosphate/nonphosphate mTOR antibody. Anti-actin antibody was used as a loading control. D, DMSO; R, rapamycin; 3, amiodarone; 4, niguldipine; 5, fluspirilene; 6, pimozide; 7, loperamide; 8, nicardipine; 9, penitrem A; 10, trifluoperazine. The concentrations of the compounds were equal to that used in the screening (SI Table 4).

and the turnover of expanded polyglutamine aggregates. We can further divide these eight compounds into two classes. The class 1 compounds consist of three FDA-approved antipsychotic drugs, fluspirilene, trifluoperazine, and pimozide. The class 2 compounds consist of five compounds, including three FDA-approved drugs for cardiovascular indications, niguldipine, nicardipine and amiodarone, that inhibit intracellular Ca^{2+} currents, loperamide, a FDA-approved drug for diarrhea, and penitrem A.

Fluspirilene is a potent diphenylbutylpiperidine antipsychotic drug, used for the treatment of schizophrenia (22). Trifluoperazine is a typical antipsychotic drug of the phenothiazine group. It is believed to exert its effect by blocking central adrenergic and dopaminergic neural transmission. Fluspirilene and trifluoperazine were found to be equally effective in the treatment of acute schizophrenic psychosis (23). Interestingly, trifluoperazine has been found to be effective in the symptomatic relief of chorea, including that of Huntington's disease patients (24). In addition, trifluoperazine, described as an inhibitor of calmodulin and mitochondrial permeability transition, can inhibit the excitotoxicity of glutamate, which has been implicated in the mechanism of neurodegeneration in Huntington's disease (25).

Pimozide is a diphenylbutylpiperidine derivative with neuroleptic properties that has been found to be useful in the management of chronic schizophrenic patients. The basic mechanism of pimozide action is believed to be related to its action on central aminergic receptors. Pimozide is used in its oral preparation in schizophrenia and chronic psychosis, Gilles de la Tourette syndrome, and resistant tics. Interestingly, in a clinical study, pimozide was found to reduce hyperkinesias associated with Huntington's disease (26).

Three compounds in the class 2, niguldipine, nicardipine, and amiodarone, are FDA-approved drugs for the treatment of cardiovascular disorders such as hypertension, angina, and cardiac arrhythmia, and are known inhibitors of intracellular Ca^{2+} current. Niguldipine is known to inhibit T-type Ca^{2+} currents in atrial myocytes. Nicardipine is a dihydropyridine calcium-channel blocking agent used for the treatment of vascular disorders such as chronic stable angina, hypertension, and Raynaud's phenomenon. Amiodarone is a highly effective antiarrhythmic drug and also has activity to block Ca^{2+} channels. In addition, trifluoperazine is known as an inhibitor of calmodulin, which recently has been proposed to regulate autophagy (11).

On the other hand, loperamide, a piperidine derivative, is an opioid receptor agonist and acts on the μ-opioid receptors in the myenteric plexus large intestines with no effect on the central nervous system because it does not cross the blood–brain barrier. Loperamide is an FDA-approved drug effective against diarrhea resulting from gastroenteritis or inflammatory bowel disease. *In vitro* culture experiments, however, show that loperamide blocks high-voltage-activated Ca^{2+} channels and *N*-methyl-D-aspartate-evoked responses in rat and mouse cultured hippocampal pyramidal neurons (27). In addition, loperamide was shown to block the action of voltage-dependent Ca^{2+} channels in cultured dorsal root ganglion neurons (28). Thus, regulation of intracellular Ca^{2+} may also be involved in the ability of loperamide to induce autophagy.

Penitrem A, a fungal neurotoxin found on ryegrass, is a selective, irreversible blocker of the high-conductance Ca^{2+}-activated K^+ (maxi-K) channel (100% block at 10 nM). Although it is not toxic to H4 cells, it exhibits *in vivo* neurotoxicity by inducing severe generalized tremors and ataxia that is associated with pathology of Purkinje cell dendrites including cytoplasmic condensation accompanied by fine vacuolation of smooth ER and enlargement of perikaryal mitochondria (29). Thus, although penitrem A is not toxic to H4 cells, it may exhibit cytotoxicity in a cell type-specific manner and not be suitable for further development as a therapeutic agent to reduce the accumulation of misfolded proteins by inducing autophagy.

Ca^{2+} is an important intracellular second messenger involved in the regulation of many cellular processes. Calmodulin is a major Ca^{2+}-binding protein and is involved in a variety of cellular functions through the activation of calmodulin-dependent enzymes, such as adenylate cyclase, phosphodiesterases, Ca^{2+}/calmodulin-dependent protein kinases, Ca^{2+}/calmodulin-dependent nitric oxide synthase, mitogen-activated protein kinase, and other protein kinases. The role of Ca^{2+} in the regulation of autophagy has been noted in recent studies. Using MCF-7 cells, Jäättelä *et al.* showed that vitamin D compounds induced both autophagy and apoptosis (30, 31). In subsequent studies, they demonstrate that elevated levels of Ca^{2+} *per se* can promote autophagy (11). Consistent with the studies of Jäättelä group, our screen also identified compounds that are known to mobilize intracellular Ca^{2+}, such as thapsigargin and A-23187, as activators of autophagy. Because thapsigargin and A-23187 also significantly increased the levels of cell death, we eliminated these compounds from further analysis. Because our screen found that multiple inhibitors of intracellular Ca^{2+} currents function as positive regulators of autophagy, we suggest the possibility that inhibition of intracellular Ca^{2+} levels may also promote autophagy.

This screen was carried out by using the H4 cell line that was derived from human neuroglioma (32). Brain tumors frequently have mutations in Pten, a dual protein/lipid phosphatase (33). The main substrate of Pten is phosphatidylinositol 3,4,5-triphosphate (PIP_3), the product of type I PI3-kinase and is inhibitory for autophagy (1). As a result of Pten mutation, brain tumors were found to have increased phosphorylated mTOR (34). Because none of the autophagy inducers identified in our work affects the status of mTOR, our work pointed out the possibility of activating autophagy downstream of mTOR in cells with increased levels of PIP_3 as a result of Pten mutations.

In summary, our work has identified eight compounds that can induce autophagic degradation and reduce the accumulation of misfolded proteins. Interestingly, other than penitrem A, all seven FDA-approved drugs showed surprisingly little toxicity in our assay, even though both rapamycin and tamoxifen had a negative impact on the cell numbers (SI Table 4). Although rapamycin has been suggested for the treatment of polyglutamine expansion diseases, the cytotoxicity of rapamycin is clearly incompatible with the goal of neuronal protection. Thus, the low cytotoxicity of the seven autophagy inducers identified in our screen provides an exciting possibility for reducing misfolded proteins without causing cellular damage. We suggest that further *in vivo* analysis of these seven FDA-approved compounds in animal models may lead to the identification of promising drugs that can be clinically tested for the treatment of human diseases characterized by the accumulation of misfolded proteins including expanded polyglutamine diseases such as Huntington's disease.

Methods

Mammalian Cell Culture and Transfection. H4 cells used for the experiments were maintained in Dulbecco's modified Eagle's medium supplemented with 10% FBS, 100 units/ml penicillin/streptomycin, and 2 mM L-glutamine (Invitrogen) at 37°C, 5% CO_2.

High-Throughput Image Analysis. H4-LC3 or H4-FYVE cells were seeded in 96-well plates and cultured in the presence of compounds for given time, then fixed with 4% paraformaldehyde (Sigma) and stained with 3 μg/ml DAPI (Sigma). Images data were collected with an ArrayScan HCS 4.0 Reader with a 20× objective (Cellomics) for DAPI-labeled nuclei and GFP/RFP-tagged intracellular proteins. The Spot Detector BioApplication was used to acquire and analyze the images after optimization. Images of 1,000 cells for each compound treatment were analyzed to obtain the average cell number per field, fluorescence spot number, area, and intensity per cell. DMSO and rapamycin were used as negative or positive control, respectively. The percentages of changes of LC3-GFP were calculated by dividing with that of DMSO-treated sam-

ples. Each treatment was done in triplicate to obtain the mean ± SD. The images were also analyzed by using a conventional fluorescence microscope for visual inspection. The experiments were repeated three times with consistent results.

Antibody Sources. The antibodies used were anti-HA antibody(Sigma), anti-phosphate/nonphosphate mTOR antibody (Cell Signaling Technology), and anti-LC3 antibody (Novus).

We thank Marta Lipinski and Dodzie Sogah for critical reading of this work. We thank Drs. Lewis Cantley (Harvard Medical School, Cambridge, MA) and Noboru Mizushima (Tokyo Medical and Dental University, Tokyo) for providing FYVE-RFP and LC3-GFP expression vectors, respectively. We thank Jennifer Waters of the Nikon Microscope Facility at the Harvard Medical School for helpful consultation. This work was supported in part by National Natural Science Foundation of China Grant 20321202, Chinese Academy of Science Grant KGCX2-SW-209 (to D.M.), and National Institute on Aging/National Institutes of Health Grant R37 AG12859 (to J. Yuan).

1. Klionsky DJ, Emr SD (2000) *Science* 290:1717–1721.
2. Levine B, Yuan J (2005) *J Clin Invest* 115:2679–2688.
3. Lum JJ, DeBerardinis RJ, Thompson CB (2005) *Nat Rev Mol Cell Biol* 6:439–448.
4. Klionsky DJ, Cregg JM, Dunn WA, Jr, Emr SD, Sakai Y, Sandoval IV, Sibirny A, Subramani S, Thumm M, Veenhuis M, Ohsumi Y (2003) *Dev Cell* 5:539–545.
5. Mizushima N, Klionsky DJ (2007) *Annu Rev Nutr* 27:19–40.
6. Kabeya Y, Mizushima N, Ueno T, Yamamoto A, Kirisako T, Noda T, Kominami E, Ohsumi Y, Yoshimori T (2000) *EMBO J* 19:5720–5728.
7. Mizushima N, Yamamoto A, Matsui M, Yoshimori T, Ohsumi Y (2004) *Mol Biol Cell* 15:1101–1111.
8. Bursch W, Ellinger A, Kienzl H, Torok L, Pandey S, Sikorska M, Walker R, Hermann RS (1996) *Carcinogenesis* 17:1595–1607.
9. Grinde B (1983) *Exp Cell Res* 149:27–35.
10. Shao Y, Gao Z, Marks PA, Jiang X (2004) *Proc Natl Acad Sci USA* 101:18030–18035.
11. Hoyer-Hansen M, Bastholm L, Szyniarowski P, Campanella M, Szabadkai G, Farkas T, Bianchi K, Fehrenbacher N, Elling F, Rizzuto R, *et al*. (2007) *Mol Cell* 25:193–205.
12. Sarbassov DD, Ali SM, Sabatini DM (2005) *Curr Opin Cell Biol* 17:596–603.
13. Demarchi F, Bertoli C, Copetti T, Eskelinen EL, Schneider C (2007) *Autophagy* 3:235–237.
14. Simonsen A, Wurmser AE, Emr SD, Stenmark H (2001) *Curr Opin Cell Biol* 13:485–492.
15. Nobukuni T, Kozma SC, Thomas G (2007) *Curr Opin Cell Biol* 19:135–141.
16. Kutateladze TG, Ogburn KD, Watson WT, de Beer T, Emr SD, Burd CG, Overduin M (1999) *Mol Cell* 3:805–811.
17. Stenmark H, Aasland R, Driscoll PC (2002) *FEBS Lett* 513:77–84.
18. Williams A, Jahreiss L, Sarkar S, Saiki S, Menzies FM, Ravikumar B, Rubinsztein DC (2006) *Curr Top Dev Biol* 76:89–101.
19. Sanchez I, Mahlke C, Yuan J (2003) *Nature* 421:373–379.
20. Wullschleger S, Loewith R, Hall MN (2006) *Cell* 124:471–484.
21. Meijer AJ, Codogno P (2004) *Int J Biochem Cell Biol* 36:2445–2462.
22. Janssen PA, Niemegeers CJ, Schellekens KH, Lenaerts FM, Verbruggen FJ, van Nueten JM, Marsboom RH, Herin VV, Schaper WK (1970) *Arzneimittelforschung* 20:1689–1698.
23. Bankier RG (1973) *J Clin Pharmacol New Drugs* 13:44–47.
24. Stokes HB (1975) *Dis Nerv Syst* 36:102–105.
25. Tang TS, Slow E, Lupu V, Stavrovskaya IG, Sugimori M, Llinas R, Kristal BS, Hayden MR, Bezprozvanny I (2005) *Proc Natl Acad Sci USA* 102:2602–2607.
26. Girotti F, Carella F, Scigliano G, Grassi MP, Soliveri P, Giovannini P, Parati E, Caraceni T (1984) *J Neurol Neurosurg Psychiatry* 47:848–852.
27. Church J, Fletcher EJ, Abdel-Hamid K, MacDonald JF (1994) *Mol Pharmacol* 45:747–757.
28. Hagiwara K, Nakagawasai O, Murata A, Yamadera F, Miyoshi I, Tan-No K, Tadano T, Yanagisawa T, Iijima T, Murakami M (2003) *Neurosci Res* 46:493–497.
29. Cavanagh JB, Holton JL, Nolan CC, Ray DE, Naik JT, Mantle PG (1998) *Vet Pathol* 35:53–63.
30. Hoyer-Hansen M, Bastholm L, Mathiasen IS, Elling F, Jäättelä M (2005) *Cell Death Differ* 12:1297–1309.
31. Mathiasen IS, Sergeev IN, Bastholm L, Elling F, Norman AW, Jäättelä M (2002) *J Biol Chem* 277:30738–30745.
32. Arnstein P, Taylor DO, Nelson-Rees WA, Huebner RJ, Lennette EH (1974) *J Natl Cancer Inst* 52:71–84.
33. Li J, Yen C, Liaw D, Podsypanina K, Bose S, Wang SI, Puc J, Miliaresis C, Rodgers L, McCombie R, *et al*. (1997) *Science* 275:1943–1947.
34. Choe G, Horvath S, Cloughesy TF, Crosby K, Seligson D, Palotie A, Inge L, Smith BL, Sawyers CL, Mischel PS (2003) *Cancer Res* 63:2742–2746.

Zhang *et al*. 10.1073/pnas.0709695104.

Supporting Information

Files in this Data Supplement:

SI Table 4
SI Table 5
SI Methods
SI Table 6

Table 4. Compounds that increase LC3-GFP$^+$ vesicles

Name	Mechanism of action	Screen conc., μM	% of control cell, no. per field	% of control LC3-GFP spot, no. per cell	% of control, LC3-GFP spot, area per cell	% of control LC3-GFP spot intensity per cell
Rapamycin	Inhibitor of mTOR	0.2	88.62 ± 1.47	205.66 ± 6.77	259.68 ± 9.92	285.38 ± 9.15
Tamoxifen	Estrogen antagonist	4.4	91.20 ± 15.79	291.52 ± 10.54	376.53 ± 9.29	585.87 ± 23.60
Grayanotoxin III*	Activator of voltage-sensitive sodium channels	6.0	129.36 ±12.25	130.17 ± 14.22	154.31 ± 12.94	210.65 ± 18.76
Loperamide*	Opioid receptor agonist; also blocks calmodulin activity, calcium channels, *N*-methyl-D-aspartate receptor channels, and maitotoxin-elicited calcium influx at higher concentrations	4.9	126.76 ± 6.52	235.49 ± 9.35	339.40 ± 16.91	666.50 ± 29.17
Amiodarone*	Na^+/Ca^{2+} exchange (NCX) inhibitor	3.7	138.50 ± 1.88	189.25 ± 17.17	236.64 ± 22.85	327.25 ± 43.47
Bay K-8644*	L-type Ca^{2+} channel agonist	7.0	134.45 ± 31.56	146.82 ± 13.80	165.46 ± 18.58	181.32 ± 24.39
Niguldipine*	L-type Ca^{2+} channel blocker	3.9	132.78 ± 18.11	282.89 ± 21.24	405.33 ± 30.57	777.92 ± 93.57
Pimozide*	T-type Ca^{2+} channel blocker	5.4	127.14 ± 5.73	218.96 ± 18.33	290.43 ± 20.62	447.75 ± 27.40

Clozapine*	Dopamine antagonist	7.7	139.18 ± 7.07	216.53 ± 0.35	275.50±0.45	350.13±4.27
Monensin*	Na^+/H^+ ionophore	3.6	92.38 ± 20.28	312.92 ± 56.28	418.31±80.64	639.29±131.46
Nigericin*	K^+/H^+ ionophore	3.4	106.90 ± 20.30	375.67 ± 20.59	551.04±33.65	747.88±59.06
Wiskostatin*	*N*-WASP inhibitor	5.9	96.96 ± 20.37	789.24 ± 32.92	1226.54±43.60	2401.38±69.13
E6 Berbamine*	Calmodulin inhibitor	3.3	131.16 ± 51.61	389.35 ± 27.58	693.82±45.62	2447.47±118.04
Paxilline*	Inhibitor of SERCA	5.7	119.79 ± 14.88	162.66 ± 11.75	185.52 ± 15.71	205.83±23.64
2,5-Ditertbutylhydroquinone*	Inhibitor of SERCA	11.3	118.42 ± 15.99	230.26 ± 10.20	269.36 ± 17.18	326.89±28.36
Cyclopiazonic acid*	An inhibitor of SERCA	7.4	112.62 ± 3.20	162.66 ± 19.27	178.53 ± 22.15	186.44±24.02
Flunarizine*	Nonselective voltage-dependent Ca^{2+} and Na^+ channels blocker	5.2	104.67 ± 23.55	155.03 ± 9.02	179.26 ± 8.59	203.66±5.56
AM 92016*	L-type calcium channel agonist	5.2	135.28 ± 14.74	166.24 ± 3.15	192.05 ± 4.63	222.83±4.66
FPL-64176*	L-type calcium channel agonist	7.2	132.45 ± 18.98	161.73 ± 4.62	180.10 ± 3.67	200.83±6.35
Verapamil*	L-type Ca^{2+} channel antagonist	5.2	132.44 ± 14.80	168.55 ± 3.31	200.63 ± 3.89	238.60±7.49
Bepridil*	Na^+/Ca^{2+} exchanger (NCX) inhibitor	6.2	111.92 ± 36.16	144.05 ± 10.37	160.34 ± 10.41	168.39±10.81
Nicardipine*	Calcium channel antagonist	4.8	131.58 ± 2.77	169.02 ± 7.41	197.46 ± 8.43	229.64±11.37
Penitrem A*	Irreversible inhibitor of high-conductance Ca^{2+}-activated K^+ (maxi-K) channel	3.9	93.08 ± 14.17	146.36 ± 9.73	163.15 ± 11.58	166.85±12.90
Propafenone*	K^+ current inhibitor	6.6	99.88 ± 10.80	210.40 ± 1.60	271.21 ± 3.18	385.97±11.98
Quinine*	K^+ channel inhibitor	6.9	115.16 ± 3.83	146.94 ± 4.24	160.38 ± 6.82	165.01±12.20
SDZ-201106*	Na^+ channel activator	5.4	94.70 ± 8.45	224.74 ± 15.83	275.43 ± 24.44	329.96±42.81
Fluspiriline*	Dopamine antagonist	5.3	143.30 ± 17.53	309.60 ± 12.26	532.51 ± 17.20	1593.16±23.32
Trifluoperazine*	Dopamine antagonist	8.3	105.72 ± 12.84	364.24 ± 23.91	520.24 ± 37.32	1010.35±109.78
TMB-8*	ER Ca^{2+} store release inhibitor	5.8	145.22 ± 28.06	170.87 ± 4.62	201.59 ± 3.89	229.50±8.36
Cyclosporin A*	Inhibitor of calcineurin and mitochondrial permeability transition	2.1	159.64 ± 24.07	155.88 ± 2.80	181.14 ± 3.22	178.79±12.89

Cypermethrin*	Calcineurin inhibitor	6.0	97.45 ± 28.70	174.74 ± 24.00	200.12 ± 35.43	208.14 ± 50.53
NapSul-Ile-Trp-CHO*	Cathepsin L inhibitor	5.1	124.74 ± 15.35	151.10 ± 5.83	172.38 ± 8.71	199.27 ± 27.78
CA-074-Me*	Cathepsin B inhibitor	6.3	132.20 ± 1.87	197.44 ± 15.66	239.20 ± 17.35	272.48 ± 13.64
E-64-d*	Calpain/cathepsin inhibitor	7.3	119.19 ± 21.97	169.98 ± 18.86	195.10 ± 25.60	244.88 ± 42.95
Ac-Leu-Leu-Nle-CHO*	Calpain inhibitor	6.5	96.31 ± 6.90	277.88 ± 24.05	362.79 ± 29.24	495.29 ± 25.66
Calpeptin*	Calpain inhibitor	6.9	128.87 ± 13.59	177.07 ± 11.10	207.34 ± 14.50	232.89 ± 14.22
Geldanamycin*	HSP-90 inhibitor	4.5	81.41 ± 1.67	313.52 ± 9.01	398.91 ± 6.37	546.80 ± 22.61
Chelerythrine*	PKC inhibitor	6.5	110.26 ± 10.99	195.46 ± 15.84	229.91 ± 21.48	213.88 ± 27.31
BADGE*	PPAR-γ antagonist	7.3	132.48 ± 3.64	156.58 ± 3.85	175.52 ± 4.86	182.11 ± 14.16
GW-9662*	PPAR-γ antagonist	9.0	105.38 ± 6.48	128.11 ± 3.42	137.98 ± 5.25	166.91 ± 16.53
Castanospermine*	Glucosidase inhibitor	13.2	157.35 ± 11.87	156.81 ± 5.77	174.29 ± 8.65	171.20 ± 10.92
Dipyridamole*	CGMP phosphodiesterase inhibitor	5.0	158.96 ± 20.49	170.20 ± 2.27	199.02 ± 1.24	213.63 ± 8.98
CAPE*	Antioxidant/NF-κB inhibitor	8.8	146.20 ± 21.95	147.15 ± 22.56	160.43 ± 26.91	150.18 ± 24.10
GM6001*	Broad-spectrum MMP inhibitor	6.4	143.94 ± 11.51	154.31 ± 13.02	171.42 ± 16.47	196.42 ± 24.22
H9*	Protein kinase inhibitor	7.71	96.70 ± 4.54	130.98 ± 12.89	139.79 ± 14.74	156.16 ± 13.15
K252A*	Protein kinase inhibitor	0.5	101.89 ± 3.64	163.88 ± 8.14	189.65 ± 9.16	215.29 ± 17.56
Indirubin*	GSK-3β inhibitor	9.5	101.26 ± 13.87	149.70 ± 11.59	158.69 ± 14.73	172.28 ± 37.92
24(*S*)-Hydroxycholesterol*	One of three major oxysterols in human circulation, liver X receptor agonist	6.2	108.20 ± 15.82	220.93 ± 16.95	299.59 ± 33.54	648.90 ± 135.44
Cyclopamine*	Inhibitor of Hedgehog pathway	6.1	110.76 ± 20.93	313.88 ± 14.53	511.72 ± 17.03	1564.12 ± 149.37
SB 202190	MAP kinase inhibitor	7.6	91.14 ± 27.00	151.97 ± 14.52	160.87 ± 14.49	169.71 ± 31.55
ML9	Inhibitor of myosin light chain kinase	6.9	82.33 ± 14.75	210.65 ± 17.98	272.31 ± 22.72	447.81 ± 36.14
Cytochalasin D	F actin capper	4.9	71.84 ± 23.37	258.44 ± 17.16	306.27 ± 24.68	378.77 ± 59.48
Bafilomycin A1	Vaculolar ATPase inhibitor	0.4	71.96 ± 7.74	691.15 ± 12.40	1608.62 ± 30.85	4027.54 ± 133.76
Tanshinone IIA	AP-1 inhibitor	8.5	79.77 ± 21.67	210.24 ± 8.21	264.51 ± 16.47	273.72 ± 21.09
Aphidicolin	Inhibitor of DNA polymerase	7.4	73.06 ± 11.61	216.53 ± 0.35	275.50 ± 0.45	350.13 ± 4.27
17-Allylaminogeldanamycin	HSP-90 inhibitor	4.3	66.89 ± 1.23	293.36 ± 24.75	364.98 ± 30.89	385.49 ± 35.56

Ikarugamycin	Inhibits clathrin-coated pit-mediated endocytosis	5.2	50.16 ± 5.27	75.79 ± 10.37	107.27 ± 4.99	172.85 ± 35.93
Latrunculin B	Inhibits actin polymerization	6.3	27.55 ± 3.99	263.28 ± 16.33	334.83 ± 21.76	723.64 ± 78.60
Trichostatin-A	Histone deacetylase inhibitor	5.2	40.15 ± 5.26	636.52 ± 62.42	864.85 ± 82.21	1649.69 ± 174.70
Thapsigargin	Inhibitor of SERCA	3.8	63.77 ± 8.62	193.06 ± 3.87	199.81 ± 2.15	187.15 ± 2.47
A-23187	Ca^{2+} ionophore	4.8	49.30 ± 3.18	181.04 ± 17.37	172.66 ± 17.40	150.83 ± 14.52
SKF-96365	Nonselective cationic channel inhibitor	6.2	42.96 ± 4.32	179.88 ± 15.61	209.11 ± 15.07	285.59 ± 17.28
Ro 31-8220	PKC inhibitor	4.5	50.58 ± 12.18	190.07 ± 6.79	190.10 ± 11.70	240.67 ± 33.17
GF-109203X	PKC inhibitor	6.1	47.77 ± 2.96	198.94 ± 8.70	208.08 ± 12.58	211.81 ± 18.29
Cytochalasin B	F actin capper	5.2	30.58 ± 18.88	208.73 ± 12.07	247.77 ± 13.55	286.43 ± 20.43
Cantharidin	PP2A inhibitor	12.7	24.47 ± 2.33	259.49 ± 24.58	332.84 ± 28.09	463.81 ± 22.89
Etoposide	Topoisomerase II inhibitor	4.3	48.17 ± 4.58	275.60 ± 33.10	306.93 ± 40.18	335.90 ± 53.85
ICRF-193	Topoisomerase II inhibitor	8.9	45.03 ± 5.04	339.59 ± 26.77	402.47 ± 35.57	483.18 ± 27.44
Furoxan	NO donor	13.4	33.47 ± 4.82	160.41 ± 18.87	178.20 ± 22.48	214.71 ± 51.52
Curcumin	NF-κB inhibitor	6.8	59.32 ± 23.06	188.94 ± 5.59	228.38 ± 5.95	249.22 ± 7.06
OBAA	Phospholipase A2 inhibitor	5.8	35.84 ± 23.94	144.80 ± 23.94	137.27 ± 17.23	155.80 ± 23.68
Z-Leu3-VS	Proteasome inhibitor	4.5	38.56 ± 5.36	141.52 ± 5.31	145.55 ± 6.88	176.02 ± 12.29

Table 5. Compounds that decrease the levels of FYVE-RFP

Name	% of control FYVE-RFP spot intensity per cell		
	2 h	4 h	8 h
LY-294002	24.99±4.60	14.79±0.76	11.09±0.69
Monensin	81.22±12.41	66.44±2.16	59.41±9.47
E6 Berbamine	59.73±19.42	54.54±7.65	58.69±8.25
Grayanotoxin III	45.44±2.32	39.37±0.46	39.83±0.38
24(*S*)-Hydroxycholesterol	38.02±0.32	38.32±3.31	38.51±8.18
Cyclopiazonic acid	41.44±9.72	30.54±15.05	33.06±1.17
2,5-Ditertbutylhydroquinone	30.41±1.88	36.58±3.73	25.02±2.97
Flunarizine	53.92±2.70	44.48±3.69	48.60±3.04
Bepridil	65.27±2.85	45.17±3.79	35.94±1.22
Cypermethrin	33.75±8.53	29.13±1.81	58.22±1.44
E-64-d	48.31±18.95	53.97±1.11	39.61±1.31

Chelerythrine	30.83±3.09	22.01±0.51	33.84±4.46
Calpeptin	58.44±3.93	63.28±1.90	61.02±2.30
Geldanamycin	35.18±4.89	41.33±1.08	39.26±3.30
BADGE	44.65±6.30	53.06±9.44	58.53±6.70
GW-9662	40.32±6.28	44.50±5.88	29.90±8.92
Castanospermine	37.35±2.44	40.02±4.97	36.45±4.89
Dipyridamole	32.22±4.36	30.25±4.52	32.54±2.22
GM6001	30.69±15.18	32.30±9.11	25.77±4.21
Indirubin	73.16±27.31	35.10±0.42	59.18±18.83

Table 6. The effects of compounds on long-lived protein degradation

	% of control long lived protein degradation			
Name	**1 h**	**2 h**	**4 h**	**24 h**
Rapamycin	159.89±11.46	171.67±10.41	149.89±24.83	165.87±4.08**
Tamoxifen	70.67±8.48	101.24±9.11	105.85±9.62	114.97±5.11*
Nigericin	91.75±6.17	88.14±4.71	96.90±4.66	95.98±5.19
Wiskostatin	68.51±3.85	90.21±1.10	92.99±4.83	97.71±2.39
Fluspiriline	93.82±3.25	143.17± 4.26	144.79±9.02	145.50±2.98**
Niguldipine	71.65±2.68	107.42±2.72	105.68±2.74	117.85±1.98**
Trifluoperazine	76.62±2.32	105.60±5.01	109.00±5.22	124.78±2.05**
Nicardipine	84.62±4.48	126.59±3.83	122.60±7.70	121.03±13.43*
Penitrem A	92.88±2.83	126.09±0.47	132.13±10.01	141.83±1.25**
Loperamide	78.70±13.17	122.10±6.48	125.21±4.29	139.19±18.77*
Amiodarone	101.32±5.95	122.42±9.71	110.75±3.68	116.73±5.54**
Pimozide	129.13±11.46	155.80±9.22	152.01±9.63	162.47±3.50**
Clozapine	115.64±11.61	125.71±8.73	115.93±4.62	119.50±11.61
Cyclopamine	91.74±6.80	111.02±4.23	109.69±0.76	103.97±4.98
Paxilline	100.56±9.22	112.34±5.20	106.67±2.89	102.35±1.49
FPL-64176	101.34±2.50	111.04±11.83	97.03±3.39	90.97±9.28
Verapamil	103.33±1.10	114.92±2.91	97.84±1.89	94.39±1.88
Propafenone	114.56±11.89	113.22±0.37	99.78±3.26	102.73±4.76
Bay K-8644	104.43±3.57	115.50±12.46	115.35±13.58	102.15±1.07
Quinine	94.35±4.48	110.94±0.54	99.32±1.64	103.56±6.09
SDZ-201106	90.63±1.10	108.53±2.11	101.77±4.86	90.03±3.35
TMB-8	106.69±4.25	124.85±10.34	109.05±8.23	95.47±1.63
Cyclosporin A	114.15±6.19	117.39±1.53	101.74±1.03	104.28±3.05
NapSul-Ile-Trp-CHO	134.83±5.67	136.94±13.25	117.24±3.08	109.40±20.83
CA-074-Me	115.20±14.85	110.18±27.65	81.00±19.27	89.11±5.44
Ac-Leu-Leu-Nle-CHO	124.56±39.39	104.95±3.82	91.35±6.76	95.45±1.36

CAPE	122.08±6.11	128.40±8.94	120.18±6.40	106.53±8.04
H9	100.94±1.02	91.55±9.42	96.55±2.55	96.19±7.00
K252A	87.00±10.58	86.53±8.23	94.70±4.83	81.16±1.11
AM 92016	95.15± 12.23	86.27±3.69	91.75±1.43	96.25±4.70
Monensin	107.28±8.23	123.64±8.45	109.16±15.17	107.54±12.08
E6 Berbamine	100.96±2.76	91.62±10.96	96.53±0.39	93.45±6.68
Cyclopiazonic acid	103.58±3.44	97.66±11.80	96.45±12.64	96.32±0.13
Grayanotoxin III	95.81±8.68	96.23±0.56	90.49±4.07	91.03±8.99
24(*S*)-Hydroxycholesterol	125.06±15.72	105.76±8.93	89.70±7.80	106.22±14.15
2,5-Ditertbutylhydroquinone	42.06±55.01	97.76±17.91	92.12±2.63	108.45±8.58
Flunarizine	97.33±4.93	107.10±21.92	93.65±12.28	113.60±3.55
Bepridil	101.90±0.46	112.64±16.40	98.78±1.92	117.59±11.71
Cypermethrin	94.75±8.49	95.28±10.79	98.36±12.63	103.75±5.39
E-64-d	84.82±13.72	76.35±0.54	79.98±11.07	91.33±9.36
Calpeptin	73.30±10.94	68.30±2.19	78.67±5.20	81.62±2.56
Geldanamycin	87.25±3.00	74.67±5.67	87.79±0.30	72.93±0.34
Chelerythrine	101.43±0.54	100.40±2.72	108.72±3.87	106.48±6.80
BADGE	96.50±12.66	84.65±6.50	95.85±9.51	91.78±6.62
GW-9662	106.33±1.88	87.58±2.53	93.22±3.05	89.29±12.14
Castanospermine	83.53±13.07	84.26±3.40	88.75±1.30	85.60±5.05
Dipyridamole	82.64±5.17	79.22±0.83	81.07±4.33	79.08±0.55
GM6001	129.48±5.05	115.08±5.17	104.88±12.67	107.46±12.17
Indirubin	105.91±6.92	94.50±1.24	95.30±11.23	100.50±3.87

The rates of long-lived protein degradation were measured as described in *Methods*. The compounds that show more than 100% of control long-lived protein degradation at 24 h were chosen to be analyzed by *t* test (**, $P < 0.02$; *, $P < 0.05$).

SI Methods

For the long-lived protein degradation assay, H4 cells were seeded in a 12-well plate for 12 h. To deplete the endogenous L-leucine pool, cells were incubated with L-leucine-free medium supplemented with dialyzed FBS for 1 h before the addition of L-leucine-free medium/dialyzed FBS containing 5 μCi/ml ^{3}H-labeled L-leucine (Amersham Pharmacia). After 24 h of incubation, the medium was replaced with the normal medium containing excess L-leucine for an additional 24 h to allow the degradation of labeled short-lived proteins. The compounds were then added, and the radioactivity was measured at 0 h, 1 h, 2 h, 4 h, and 24 h after the addition of the compounds using a liquid scintillation counter. The cell lysates were collected at 24 h for the measurement of radioactivity. The rates of degradation were obtained by dividing the average cpm in medium with the total cpm (= cpm in the medium + cpm in the lysate). The degradation rates of compound treated samples were divided by that of DMSO-treated samples to obtain the percentage of changes.